Hybrid Adaptive Control for the DC-DC Boost Converter ⋆

Ryan S. Johnson* Berk Altin Ricardo G. Sanfelice*****

University of California, Santa Cruz, CA 95060 USA
*(e-mail:*rsjohnso@ucsc.edu,**berkaltin@ucsc.edu,***ricardo@ucsc.edu).*

Abstract: In this paper, we consider the problem of practically asymptotically stabilizing the DC-DC boost converter under parameter uncertainty. In particular, we propose an estimation algorithm that identifies the input voltage and output load of the converter in finite time. Using these estimates, we design a control algorithm that "unites" global and local control schemes. The global control scheme induces practical asymptotic stability of a desired output voltage and corresponding current, and the local control scheme maintains industry-standard PWM behavior during steady state. Stability properties for the resulting hybrid closed-loop system are established and simulation results illustrating the main results are provided.

Keywords: Electrical circuits, energy and power networks, hybrid inclusions, cyber-physical systems, switched systems, learning, identification, stabilization, modeling.

1. INTRODUCTION

The DC-DC boost converter is widely used in the power systems of electric vehicles (Bellur and Kazimierczuk, 2007). These systems operate under constantly changing demands such as supplying energy during acceleration and storing it during braking, necessitating power conversion technology that is capable of adapting to these changes. The industry standard control scheme for the boost converter is pulse-width modulation (PWM). However, since PWM controllers typically utilize a linearized model of the converter dynamics, the stability properties only hold locally near the set-point (Kassakian et al., 1991). Recently, a renewed interest in power converters has originated from the rise of hybrid modeling paradigms and new perspectives on their control, including time-based switching, state-event triggered control, and optimization-based control, were proposed (Vasca and Iannelli, 2012).

In this paper, motivated by the prevalence of PWM control implementations in industry and the widespread familiarity with its operation, we propose a control algorithm that stabilizes the boost converter even under uncertainty in the input voltage and load resistance and maintains PWM behavior during steady-state operation. We utilize the modeling approach first proposed by Theunisse et al. (2015) that captures the transient behavior and every possible state of the converter system. Using hybrid systems tools presented in Section 2, we study the properties of a modular "uniting" control framework, discussed in Section 3, that switches between global and local control schemes. In Section 4, we propose an estimator that permits finite-time estimation of the converter input voltage and load resistance. We show in Section 5 that the closed-loop uniting framework and finite-time estimator induce global practical asymptotic stability of a desired voltage value. The hybrid systems tools recently developed in (Goebel et al., 2012, Sanfelice, 2021) form the enabling techniques to achieve these results. Due to space constraints, some proofs are sketched or omitted, and will be published elsewhere.

Notation. We denote the real, nonnegative, positive, and natural numbers as $\mathbb{R}$, $\mathbb{R}_{\geq 0}$, $\mathbb{R}_{>0}$, and $\mathbb{N}$, respectively. Given a set S, ∂S denotes its boundary and $\overline{S}$ its closure. The Euclidean norm is denoted $|\cdot|$. The distance of a point x to a nonempty set S is defined by $|x|_S = \inf_{y\in S}|y-x|$. Given a set-valued mapping $M : \mathbb{R}^m \rightrightarrows \mathbb{R}^n$, the domain of M is the set $\operatorname{dom} M = \{x \in \mathbb{R}^m \ : \ M(x) \neq \varnothing\}$, and the range of M is the set $\operatorname{rge} M = \{y \in \mathbb{R}^n : \exists x \in \mathbb{R}^m \ s.t.\ y \in M(x)\}$. A function $\beta : \mathbb{R}_{\geq 0} \times \mathbb{R}_{\geq 0} \to \mathbb{R}_{\geq 0}$ is said to be of class $\mathcal{KL}$ if it is nondecreasing in its first argument, nonincreasing in its second argument, $\lim_{r\to 0+}\beta(r,s) = 0$ for each $s \in \mathbb{R}_{\geq 0}$, and $\lim_{s\to\infty}\beta(r,s) = 0$ for each $r \in \mathbb{R}_{\geq 0}$. The μ-sublevel set of the function $V \ : \ \operatorname{dom} V \to \mathbb{R}_{\geq 0}$, which is the set of points $\{x \in \operatorname{dom} V \ : \ V(x) \leq \mu\}$, is denoted $L_V(\mu)$. The closed unit ball centered at the origin of appropriate dimension (in the Euclidean norm) is denoted $\mathbb{B}$. The set $\mathcal{SP}^{n\times n}$ contains positive semidefinite matrices with dimension $n \times n$.

2. PRELIMINARIES

2.1 Preliminaries on hybrid systems

In this paper, a hybrid system $\mathcal{H}$ has data (C, F, D, G, κ) and is given by (Goebel et al., 2012, Sanfelice, 2021)

$$\mathcal{H} = \begin{cases} (x,u) \in C & \dot{x} \ \in F(x,u) \\ (x,u) \in D & x^+ \in G(x,u) \\ & \quad y = \kappa(x,u) \end{cases} \tag{1}$$

where $x \in \mathbb{R}^n$ is the state, $u \in \mathbb{R}^m$ is the input, $F : \mathbb{R}^n \times \mathbb{R}^m \rightrightarrows \mathbb{R}^n$ is a set-valued map defining the flow map of the

⋆ Research partially supported by NSF Grants no. ECS-1710621 and CNS-1544396, by AFOSR Grants no. FA9550-16-1-0015, FA9550-19-1-0053, and FA9550-19-1-0169, by CITRIS and the Banato Institute at the University of California, and by the ARCS Foundation.

differential inclusion capturing the continuous dynamics, and $C \subset \mathbb{R}^n \times \mathbb{R}^m$ defines the flow set on which flows are permitted. Similarly, $G : \mathbb{R}^n \times \mathbb{R}^m \rightrightarrows \mathbb{R}^n$ is a set-valued map defining the jump map of the difference inclusion modeling the discrete behavior, and $D \subset \mathbb{R}^n \times \mathbb{R}^m$ is the jump set on which jumps are permitted. The vector $y \in \mathbb{R}^n$ defines the output of the hybrid system.

A solution x to $\mathcal{H}$ is parameterized by $(t, j) \in \mathbb{R}_{\geq 0} \times \mathbb{N}$, where t is the amount of ordinary time that has passed and j is the number of jumps that have occurred. The domain of x, denoted $\operatorname{dom} x \subset \mathbb{R}_{\geq 0} \times \mathbb{N}$, is a hybrid time domain, in the sense that for every $(T, J) \in \operatorname{dom} x$, there exists a nondecreasing sequence $\{t_j\}_{j=0}^{J+1}$ with $t_0 = 0$ such that $\operatorname{dom} x \cap ([0, T] \times \{0, 1, \ldots, J\}) = \bigcup_{j=0}^{J} ([t_j, t_{j+1}], \{j\})$. A solution x to $\mathcal{H}$ is called maximal if it cannot be extended. A solution is called complete if its domain is unbounded. The set of all maximal solutions to $\mathcal{H}$ is denoted $\mathcal{S}_{\mathcal{H}}$, and the set of all maximal solutions to $\mathcal{H}$ with initial condition belonging to a set K is denoted $\mathcal{S}_{\mathcal{H}}(K)$. A set K is said to be forward invariant for $\mathcal{H}$ if every solution $x \in \mathcal{S}_{\mathcal{H}}(K)$ is complete and satisfies $\operatorname{rge} x \subset K$.

2.2 Boost converter model

The boost converter is a class of switched-mode power supply that utilizes a switch S, inductor L, diode d, and capacitor c to raise the voltage at the output load R compared to the input voltage E. The state of the switch S (open or closed) represents the control input to the boost converter plant. When the switch is closed, current flows through the inductor and generates a magnetic field. When the switch is opened, the inductor magnetic field decays to maintain the current towards the load, causing a polarity reversal within the inductor. The primary voltage source in series with the inductor then charges the capacitor through the diode to a higher voltage than is attainable using the voltage source alone. If the switch is cycled fast enough, the inductor does not fully discharge between cycles and the load voltage remains higher than that of the source.

The boost converter dynamics may be expressed as a (continuous time) plant, $\mathcal{H}_P$, with discrete-valued input denoting the position of the switch S. We model it as $\mathcal{H}$ in (1) but with no jumps. That is, $\mathcal{H}_P$ with state $x := (v_c, i_L)$, $x \in \mathcal{X}_P := \widetilde{M}_0 \cup \widetilde{M}_1$ which are given below, input $q \in \{0, 1\}$, and output given by x. Following Theunisse et al. (2015), its dynamics reduce to the differential inclusion with constraints

$$\dot{x} \in F_P(x, q) \qquad (x, q) \in C_P \tag{2}$$

where $C_P := (\widetilde{M}_0 \times \{0\}) \cup (\widetilde{M}_1 \times \{1\})$, $\widetilde{M}_0 := \overline{M_1} \cup \overline{M_3} = \{x \in \mathbb{R}^2 : i_L \geq 0\}$, $\widetilde{M}_1 := M_2 = \{x \in \mathbb{R}^2 : v_c \geq 0\}$ with $M_1 = \{x \in \mathbb{R}^2 : i_L > 0\} \cup \{x \in \mathbb{R}^2 : v_c \leq E, i_L = 0\}$, $M_2 = \{x \in \mathbb{R}^2 : v_c \geq 0\}$, $M_3 = \{x \in \mathbb{R}^2 : v_c > E, i_L = 0\}$, and F_P is the Krasovskii regularization of the vector fields and the corresponding constraint sets associated with each mode of circuit operation given by, for each $x \in \mathcal{X}_P$, (see Theunisse et al. (2015) for details)

$$F_P(x, 0) := \begin{cases} \begin{bmatrix} -\frac{1}{Rc} v_c + \frac{1}{c} i_L \\ -\frac{1}{L} v_c + \frac{E}{L} \end{bmatrix} & \text{if } x \in \overline{M_1} \setminus \overline{M_3} \\ \left\{-\frac{1}{Rc} v_c\right\} \times \left[-\frac{1}{L} v_c + \frac{E}{L}, 0\right] & \text{if } x \in \overline{M_3} \end{cases} \tag{3}$$

$$F_P(x, 1) := \begin{bmatrix} -\frac{1}{Rc} v_c \\ \frac{E}{L} \end{bmatrix} \qquad \text{if } x \in \widetilde{M}_1.$$

3. MOTIVATION AND PROBLEM STATEMENT

Since the supply voltage E and load resistance R for the converter may vary during operation, it is desirable to estimate these values so the chosen control algorithm can adapt accordingly. Furthermore, since the stability properties of boost converter PWM control algorithms typically only hold locally near the set-point, we desire to solve the following problems:

> **Problem 1:** Design an algorithm that permits online estimation of the boost converter input voltage E and load resistance R.
> **Problem 2:** Design an adaptive control law whose closed-loop system induces practical asymptotic stability of a desired output voltage.

Due to our desire to maintain PWM operation in steady-state, the boost converter is an ideal candidate for the control framework known as "uniting control." This framework utilizes a divide and conquer approach to control design by combining two feedback controllers and a logic-based algorithm that selects which controller to apply. Uniting control strategies permit combining a global controller that renders a set-point stable but may not have good performance near the set point, and a local controller that induces satisfactory performance, but only locally (Teel and Kapoor, 1997).

The uniting control logic is implemented as follows. Given a plant $\mathcal{H}_P$ as in (2) interconnected with two separate control algorithms, $\mathcal{H}_0$, referred to as "global," and $\mathcal{H}_1$, referred to as "local," the choice of control algorithm is governed by a supervisory controller that selects between $\mathcal{H}_1$ and $\mathcal{H}_0$ based on the plant state in relation to a closed set $\mathcal{N}$ and an open set $\mathcal{M} \supset \mathcal{N}$ as follows:

- Apply the global controller $\mathcal{H}_1$ until the solution to the plant enters $\mathcal{N}$. When any such point is reached, switch to the local controller $\mathcal{H}_0$.
- Apply the local controller $\mathcal{H}_0$ as long as the solution to the plant remains inside $\mathcal{M}$. If the state of the plant leaves $\mathcal{M}$, switch to the global controller $\mathcal{H}_1$.

Given $\mathcal{H}_1$ and $\mathcal{H}_0$, the uniting control sets $\mathcal{N}$ and $\mathcal{M}$ will be designed to satisfy the following assumption.

Assumption 3.1. *Given a hybrid system $\mathcal{H}_P$ as in* (2)*,*

- *each maximal solution x to $\mathcal{H}_P$ with input q generated by $\mathcal{H}_1$ converges to $\mathcal{N}$ in finite (hybrid) time;*
- *each solution x to $\mathcal{H}_P$ from $\mathcal{N}$ and input q generated by $\mathcal{H}_0$ remains in $\mathcal{M}$ for all (hybrid) time.*

Hence, for the boost converter, the global controller drives the converter state into $\mathcal{N}$, from where solutions under the local PWM controller remain inside $\mathcal{M}$ for all future time.

Next, we will separately design the parameter estimation algorithm and the global and local control algorithms before combining them using the uniting control framework.

4. HYBRID PARAMETER ESTIMATION AND UNITING CONTROL

4.1 Parameter estimation

We begin by studying Problem 1 from Section 3. For the purpose of estimating R and E, we establish the following lemma, which allows us to express the dynamics of maximal solutions to $\mathcal{H}_P$ in a convenient form.

Lemma 4.1. *Each maximal solution $t \mapsto x(t)$ to $\mathcal{H}_P$ in (2) with input $t \mapsto q(t)$ satisfies*[1]

$$\dot{x}(t) = f_1(x(t), q(t)) + f_2(x(t), q(t))\vartheta \tag{4}$$

for all $t \in \operatorname{dom}(x, q)$, where $\vartheta = (\vartheta_1, \vartheta_2) := (R^{-1}, E)$ and

$$f_1(x,q) := \begin{cases} \begin{bmatrix} \frac{i_L}{c} \\ -\frac{v_c}{L} \end{bmatrix} & \text{if} \quad q = 0,\ x \in \overline{M_1} \setminus \overline{M_3} \\ \begin{bmatrix} 0 \\ 0 \end{bmatrix} & \text{if} \quad (q = 1,\ x \in \widetilde{M_1}) \text{ or } (q = 0,\ x \in \overline{M_3}) \end{cases}$$

$$f_2(x,q) := \begin{cases} \begin{bmatrix} -\frac{v_c}{c} & 0 \\ 0 & \frac{1}{L} \end{bmatrix} & \text{if} \quad (q = 0,\ x \in \overline{M_1} \setminus \overline{M_3}) \text{ or } (q = 1,\ x \in \widetilde{M_1}) \\ \begin{bmatrix} -\frac{v_c}{c} & 0 \\ 0 & 0 \end{bmatrix} & \text{if} \quad q = 0,\ x \in \overline{M_3}. \end{cases}$$

Estimating the parameters R and E is equivalent to estimating the parameter vector ϑ in (4). For this purpose, we extend the finite-time parameter estimator proposed in Hartman et al. (2012) to classes of hybrid systems whose solutions satisfy (4). The algorithm is expressed as a hybrid system, denoted $\mathcal{H}_E$, and operates as follows. Let $(t, j) \mapsto z_E(t, j)$ be a solution to $\mathcal{H}_E$ – hence, defined on a hybrid time domain – with $z_E = (\hat{x}, \hat{\theta}, \omega, Q, \eta, \Gamma)$, where $\hat{x}$ is the estimate of x, $\hat{\vartheta}$ is the estimate of ϑ, and ω, Q, η, Γ are auxiliary variables. Consider the initial interval of flow $I^0 := [t_0, t_1] \times \{0\}$ for the solution z_E with constant ϑ and initial conditions $\omega(0,0) = 0$, $Q(0,0) = 0$, $\eta(0,0) = 0$, $\Gamma(0,0) = 0$, and $\hat{\vartheta}(0,0)$ arbitrary. Omitting the (t, j) of solutions, for the sake of making an argument, suppose that over this interval of flow, Q and Γ satisfy

$$\dot{Q} = \omega^\top \omega, \qquad \dot{\Gamma} = \omega^\top \omega \vartheta. \tag{5}$$

Then, if there exists a positive time $t_1 \in I^0$ such that $Q(t_1, 0)$ is invertible, $\hat{\vartheta}$ can be reset to $Q^{-1}\Gamma$, leading to

$$\hat{\vartheta}(t_1, 1) = Q^{-1}(t_1, 0)\Gamma(t_1, 0) \tag{6}$$
$$= \left(\int_0^{t_1} \omega(t,0)^\top \omega(t,0) dt\right)^{-1} \left(\int_0^{t_1} \omega(t,0)^\top \omega(t,0) dt \vartheta\right) = \vartheta.$$

However, since ϑ is unknown prior to hybrid time $(t_1, 1)$, a trajectory for Γ satisfying (5) cannot be generated. Due to this, we rewrite the dynamics of Γ as

$$\dot{\Gamma} = \omega^\top(\omega\hat{\vartheta} + x - \hat{x} - \eta)$$

where $\eta = x - \hat{x} - \omega(\vartheta - \hat{\vartheta})$. Note that since $\omega(0,0) = 0$, the initial condition $\eta(0,0) = 0$ implies $\hat{x}(0,0) = x(0,0)$. Differentiating η yields

$$\dot{\eta} = \dot{x} - \dot{\hat{x}} - \dot{\omega}(\vartheta - \hat{\vartheta}) + \omega\dot{\hat{\vartheta}}. \tag{7}$$

Next, we define a matrix function $(x, q) \mapsto K(x, q) = K^\top(x, q) > 0$ to be designed. The arguments of K are omitted below for simplicity. Then, let $\hat{x}$, ω, and $\hat{\vartheta}$ satisfy

$$\dot{\hat{x}} = f_1(x, q) + f_2(x, q)\hat{\vartheta} + K(x - \hat{x}) + \omega\dot{\hat{\vartheta}}$$
$$\dot{\omega} = f_2(x, q) - K\omega.$$

Plugging the above expressions into (7) yields $\dot{\eta} = -K\eta$. Hence, ω, Q, η, and Γ are now expressed in terms of known quantities and we can compute $\hat{\vartheta}$ as in (6).

[1] Since $\mathcal{H}_P$ in (2) is a continuous-time system, its solutions are parameterized using only t.

Following Hartman et al. (2012), we implement the estimation scheme outlined above as a hybrid algorithm whose jump map imposes the initial conditions specified just above (5) and computes $\hat{\vartheta}$ as in (6). Then, the hybrid system $\mathcal{H}_E = (C_E, F_E, D_E, G_E, \hat{\theta})$ has state $z_E := (\hat{x}, \hat{\vartheta}, \omega, Q, \eta, \Gamma) \in \mathcal{X}_E := \mathbb{R}^2 \times \mathbb{R}^2 \times \mathbb{R}^{2\times 2} \times \mathcal{SP}^{2\times 2} \times \mathbb{R}^2 \times \mathbb{R}^2$, inputs $(x, q) \in C_P$, output $\hat{\theta} \in \mathbb{R}^2_{>0}$, and dynamics

$$\begin{aligned} \dot{z}_E &= F_E(x, q, z_E) & (x, q, z_E) &\in C_E \\ z_E^+ &= G_E(x, z_E) & (x, q, z_E) &\in D_E \\ \hat{\theta} &:= (\hat{\vartheta}_1^{-1}, \hat{\vartheta}_2) = (\hat{R}, \hat{E}) \end{aligned} \tag{8}$$

where $G_E(x, z_E) := (x, Q^{-1}\Gamma, 0, 0, 0, 0)$,

$$F_E(x, q, z_E) := \begin{bmatrix} f_1(x,q) + f_2(x,q)\hat{\vartheta} + K(x - \hat{x}) + \omega h(x, q, z_E) \\ h(x, q, z_E) \\ f_2(x, q) - K\omega \\ \omega^\top \omega \\ -K\eta \\ \omega^\top(\omega\hat{\vartheta} + x - \hat{x} - \eta) \end{bmatrix}$$

with $h(x, q, z_E) = \Omega(\omega^\top + f_2(x, q)^\top)(x - \hat{x})$, and

$$C_E := \{(x, q, z_E) \in C_P \times \mathcal{X}_E : \det(Q) \le \mu\}$$
$$D_E := \{(x, q, z_E) \in C_P \times \mathcal{X}_E : \det(Q) \ge \mu\}.$$

The matrix function K and the parameter $\Omega = \Omega^\top > 0$ modify the convergence rate of $\hat{x}$ and $\hat{\vartheta}$ during flows, and $\mu > 0$ ensures that Q^{-1} is well-defined in the jump map.

The dynamics of $\mathcal{H}_E$ in (8) are similar to the estimator proposed in Hartman et al. (2012). However, in Hartman et al. (2012), f_1 and f_2 are continuous functions of the state and input, compared to piecewise continuous in (4).

Similarly to Hartman et al. (2012), each maximal solution to $\mathcal{H}_E$ is guaranteed to jump if the following holds.

Assumption 4.2. *Given a compact set $\Lambda \subset \mathcal{X}_P \times \{0, 1\}$, there exist $a, b > 0$ such that, for any maximal solution $t \mapsto x(t)$ to $\mathcal{H}_P$ with input $t \mapsto q(t)$ satisfying $\operatorname{rge}(x, q) \subset \Lambda$ and any $\tilde{t} > 0$ such that $[\tilde{t}, \tilde{t} + a] \subset \operatorname{dom}(x, q)$,*

$$\int_{\tilde{t}}^{\tilde{t}+a} f_2(x(s), q(s))^\top f_2(x(s), q(s)) ds \ge bI. \tag{9}$$

Next, we establish the following proposition, which states the stability properties of the interconnection of the plant $\mathcal{H}_P$ and estimator $\mathcal{H}_E$. The proof follows similarly to (Li and Sanfelice, 2019, Proposition 4.4).

Proposition 4.3. *Consider the interconnection of $\mathcal{H}_P$ in (2) and $\mathcal{H}_E$ in (8) with $K(x, q) = k + \frac{1}{4} f_2(x, q)\Omega f_2^\top(x, q)$ where $k > \frac{1}{4}I$ and $\Omega = \Omega^\top > 0$, with input*[2] *$(t, j) \mapsto q(t, j) \in \{0, 1\}$. Given a compact set $\Lambda \subset \mathcal{X}_P \times \{0, 1\}$ satisfying Assumption 4.2, there exists $\mu > 0$ in (8) such that, for each maximal solution $\phi = (x, q, z_E)$ to the interconnection satisfying $\operatorname{rge}(x, q) \subset \Lambda$, there exists a hybrid time $(t', j') \in \operatorname{dom} \phi$ such that $\phi(t', j') \in \Lambda \times \mathcal{A}_E$ with*

$$\mathcal{A}_E := \{z_E \in \mathcal{X}_E : \hat{x} = x,\ \hat{\vartheta} = \vartheta,\ \eta = 0\}. \tag{10}$$

4.2 Global control algorithm

Next we study Problem 2 from Section 3 in the context of the uniting control framework described therein, beginning with the global control algorithm. The hybrid control

[2] Since the interconnection of $\mathcal{H}_P$ and $\mathcal{H}_E$ is a hybrid system, the input and state of $\mathcal{H}_P$ are now parameterized by (t, j).

algorithm proposed in Theunisse et al. (2015) represents an ideal candidate for the global controller. Given a desired output voltage v_c^*, this algorithm renders the set

$$\mathcal{A}_P := \{x \in \mathbb{R}^2 : v_c = v_c^*, i_L = i_L^* = \tfrac{v_c^{*2}}{RE}\} \tag{11}$$

globally asymptotically stable for the boost converter when the converter parameters $c, L, R, E > 0$ are known.

However, in contrast to Theunisse et al. (2015), the parameters R and E are unknown in this paper. Hence, we apply the certainty equivalence principle and substitute the parameter estimates $\hat{R}$ and $\hat{E}$ from $\mathcal{H}_E$ in (8) for R and E, respectively. Then, following the derivation in Theunisse et al. (2015), given a desired voltage v_c^*, the set-point $x^*(\hat{\theta}) := (v_c^*, \hat{i}_L^*)$ with $\hat{i}_L^* := \frac{v_c^{*2}}{\hat{R}\hat{E}}$ is stabilized using the control Lyapunov function $V(x,\hat{\theta}) = (x - x^*(\hat{\theta}))^\top P(x - x^*(\hat{\theta}))$, where $P = \left[\begin{smallmatrix} p_{11} & 0 \\ 0 & p_{22}\end{smallmatrix}\right] > 0$ with $\frac{p_{11}}{c} = \frac{p_{22}}{L}$. We define a hybrid system $\mathcal{H}_1$ with state $z_1 := q \in \mathcal{X}_1 := \{0,1\}$, inputs $x \in \mathcal{X}_P$ and $\hat{\theta} \in \mathbb{R}^2_{>0}$, and dynamics

$$\begin{aligned} \dot{q} &= 0 =: F_1(z_1) && (x, z_1, \hat{\theta}) \in C_1 \\ q^+ &= 1 - q =: G_1(z_1) && (x, z_1, \hat{\theta}) \in D_1 \\ \kappa_1(x, z_1, \hat{\theta}) &:= q \end{aligned} \tag{12}$$

where κ_1 represents the input q of $\mathcal{H}_P$,

$$\begin{aligned} C_1 &:= \left\{(x, z_1, \hat{\theta}) \in \mathcal{X}_P \times \mathcal{X}_1 \times \mathbb{R}^2_{>0} : \tilde{\gamma}_0(x,\hat{\theta}) \le \rho, q = 0\right\} \\ &\quad \cup \left\{(x, z_1, \hat{\theta}) \in \mathcal{X}_P \times \mathcal{X}_1 \times \mathbb{R}^2_{>0} : \tilde{\gamma}_1(x,\hat{\theta}) \le \rho, q = 1\right\} \\ D_1 &:= \left\{(x, z_1, \hat{\theta}) \in \mathcal{X}_P \times \mathcal{X}_1 \times \mathbb{R}^2_{>0} : \tilde{\gamma}_0(x,\hat{\theta}) \ge \rho, q = 0\right\} \\ &\quad \cup \left\{(x, z_1, \hat{\theta}) \in \mathcal{X}_P \times \mathcal{X}_1 \times \mathbb{R}^2_{>0} : \tilde{\gamma}_1(x,\hat{\theta}) \ge \rho, q = 1\right\}, \end{aligned}$$

and $\rho \in \mathbb{R}_{>0}$ is a design parameter that, as in Theunisse et al. (2015), spatially regularizes the closed-loop global controller by modifying the separation between the functions $\tilde{\gamma}_0$ and $\tilde{\gamma}_1$ to avoid Zeno behavior. The functions $\tilde{\gamma}_q$, $q \in \{0,1\}$ are given by

$$\tilde{\gamma}_q(x,\hat{\theta}) := \gamma_q(x,\hat{\theta}) + K_q(v_c - v_c^*)^2 \tag{13}$$

where $\gamma_q(x,\hat{\theta}) := 2(a_q v_c^2 + b_q v_c + c_q i_L + d_q)$ with

$a_0 = -\frac{p_{11}}{\hat{R}c}$, $a_1 = -\frac{p_{11}}{\hat{R}c}$, $b_0 = \frac{p_{11}v_c^*}{\hat{R}c} + \frac{p_{22}\hat{i}_L^*}{L}$,
$b_1 = \frac{p_{11}v_c^*}{\hat{R}c}$, $c_0 = -\frac{p_{11}v_c^*}{c} + \frac{p_{22}\hat{E}}{L}$, $c_1 = \frac{p_{22}\hat{E}}{L}$,
$d_0 = -\frac{p_{22}\hat{i}_L^*\hat{E}}{L}$, $d_1 = -\frac{p_{22}\hat{i}_L^*\hat{E}}{L}$,

and $K_0 = k_0\frac{2p_{11}}{\hat{R}c}$, $K_1 = k_1\frac{2p_{11}}{\hat{R}c}$, where $k_0, k_1 \in (0,1)$ are design parameters that ensure $K_0, K_1 \in (0, 2p_{11}/(\hat{R}c))$.

Given $(t,j) \mapsto x(t,j)$ and $(t,j) \mapsto \hat{\theta}(t,j)$, each solution $(t,j) \mapsto q(t,j)$ to $\mathcal{H}_1$ maintains a constant switch state until $x(t,j)$ intersects with the ρ level-set of $\tilde{\gamma}_q$, at which point the value of q is toggled.

Note that the jump set D_1 below (12) has been modified compared to the model in Theunisse et al. (2015). In particular, the conditions $\tilde{\gamma}_0(x,\hat{\theta}) = \rho$ and $\tilde{\gamma}_1(x,\hat{\theta}) = \rho$ in Theunisse et al. (2015) are instead $\tilde{\gamma}_0(x,\hat{\theta}) \ge \rho$ and $\tilde{\gamma}_1(x,\hat{\theta}) \ge \rho$, respectively. This change ensures completeness of maximal solutions for the closed-loop uniting control algorithm discussed in Section 4.4.

To ensure that Assumption 4.2 is satisfied for the closed-loop global controller, we define the set

$$\Pi := \{x \in \mathcal{X}_P : v_c > 0, i_L > 0\}. \tag{14}$$

Then, we establish the following proposition, which states the stability properties of the closed-loop global controller.

Proposition 4.4. *Consider the interconnection of the plant $\mathcal{H}_P$ in (2) with $c, L, R, E > 0$, global controller $\mathcal{H}_1$ in (12) with $k_0, k_1 \in (0,1)$ and $\rho > 0$, and parameter estimator $\mathcal{H}_E$ in (8) with $K(x,q) = k + \frac{1}{4}f_2(x,q)\Omega f_2^\top(x,q)$, where $k > \frac{1}{4}I$ and $\Omega = \Omega^\top > 0$. Given a desired set-point voltage $v_c^* > E$ and a compact set $\Delta \subset \Pi \times \mathcal{X}_1 \times \mathcal{X}_E$, with Π given in (14), that is forward invariant for the interconnection, there exists $\mu > 0$ in (8) such that, for each maximal solution $\phi = (x, z_1, z_E)$ to the interconnection with $\phi(0,0) \in \Delta$, there exists a hybrid time $(t', j') \in \operatorname{dom}\phi$ such that $\phi(t', j') \in \Pi \times \mathcal{X}_1 \times \mathcal{A}_E$, with $\mathcal{A}_E$ given in (10). Furthermore, there exists $\beta \in \mathcal{KL}$ such that, for each compact set $\Upsilon \subset \mathbb{R}^2$ and each $\nu > 0$, there exists $\rho^* > 0$ guaranteeing the following property: for each $\rho \in (0, \rho^*]$ defining C_1 and D_1 in (12), every solution ϕ to the interconnection with $\phi(0,0) \in \Upsilon \times \mathcal{X}_1 \times \mathcal{A}_E$ is such that, for all $(t,j) \in \operatorname{dom}\phi$, its x component satisfies*

$$|x(t,j)|_{\mathcal{A}_P} \le \beta(|x(0,0)|_{\mathcal{A}_P}, t + j) + \nu. \tag{15}$$

Sketch of Proof: Assumption 4.2 holds for every maximal solution with $\phi(0,0) \in \Delta$. Then, from Proposition 4.3 we have $\hat{\theta} = \theta$ in finite time, and the stability result follows from (Theunisse et al., 2015, Theorem IV.7). □

In words, Proposition 4.4 states that, for each maximal solution to the closed-loop system resulting with the global controller from Δ, the parameter estimate $\hat{\theta}$ converges to θ in finite time. Then, following convergence of $\hat{\theta}$, solutions satisfy the practical $\mathcal{KL}$ stability condition given in (15).

4.3 Local control algorithm

Next, we design the local control algorithm for the uniting control framework. Recall from Section 3 that we desire to maintain PWM behavior near the set-point. Assuming the converter operates only in the continuous conduction mode, we design the PWM controller by averaging the converter dynamics as in Teel and Nešić (2010). The average system for the steady-state converter is given by

$$\dot{x} = A_0(\hat{\theta})x + B_0(\hat{\theta}) + d(x,\hat{\theta})(A_1(\hat{\theta}) - A_0(\hat{\theta}))x \tag{16}$$

where the function d represents the PWM duty cycle and

$$A_0(\hat{\theta}) = \begin{bmatrix} -\frac{1}{\hat{R}c} & \frac{1}{c} \\ -\frac{1}{L} & 0 \end{bmatrix}, \quad A_1(\hat{\theta}) = \begin{bmatrix} -\frac{1}{\hat{R}c} & 0 \\ 0 & 0 \end{bmatrix}, \quad B_0(\hat{\theta}) = \begin{bmatrix} 0 \\ \frac{\hat{E}}{L} \end{bmatrix}.$$

Next, we linearize (16) about $x^*(\hat{\theta})$ (see Kassakian et al. (1991) for details) and denote the region of the state-space where the linearization holds as $\mathcal{L} \subset \mathbb{R}^2$. Expressing the linearized average model in error coordinates yields

$$\dot{\tilde{x}} = A_{\text{avg}}(\hat{\theta})\tilde{x} + B_{\text{avg}}(\hat{\theta})\tilde{d}(x,\hat{\theta}) \tag{17}$$

where $\tilde{x} = x - x^*(\hat{\theta})$ and $\tilde{d}(x,\hat{\theta}) = d(x,\hat{\theta}) - d^*(\hat{\theta})$, with $d^*(\hat{\theta}) = 1 - \hat{E}/v_c^*$ being the steady-state duty cycle for the linearized average model, and

$$A_{\text{avg}}(\hat{\theta}) = \begin{bmatrix} -\frac{1}{\hat{R}c} & \frac{\hat{E}}{v_c^* c} \\ -\frac{\hat{E}}{v_c^* L} & 0 \end{bmatrix}, \qquad B_{\text{avg}}(\hat{\theta}) = \begin{bmatrix} -\frac{v_c^{*2}}{\hat{R}\hat{E}c} \\ \frac{v_c^*}{L} \end{bmatrix}.$$

Since the pair $(A_{\text{avg}}, B_{\text{avg}})$ is controllable for all $\hat{R}, \hat{E} > 0$, we apply a full state-feedback controller of the form

$$\tilde{d}(x,\hat{\theta}) = -\widetilde{K}(\hat{\theta})\tilde{x}, \tag{18}$$

yielding the closed-loop dynamics

$$\dot{\tilde{x}} = A_{\rm cl}(\hat{\theta})\tilde{x} \tag{19}$$

where $\widetilde{K}$ is chosen such that $A_{\rm cl}(\hat{\theta}) := A_{\rm avg}(\hat{\theta}) - B_{\rm avg}(\hat{\theta})\widetilde{K}(\hat{\theta})$ is Hurwitz for each $\hat{\theta}$. Then, the PWM duty cycle is computed as $d(x,\hat{\theta}) := \psi(d^*(\hat{\theta}) - \widetilde{K}(\hat{\theta})\tilde{x})$, where $\psi(s) := \min\{\max\{0,s\},1\}$ is a saturation function.

Then, we define the hybrid system $\mathcal{H}_0$ with state $z_0 := \tau \in \mathcal{X}_0 := [0,1]$, inputs $x \in \mathcal{X}_P$ and $\hat{\theta} \in \mathbb{R}^2_{>0}$, and dynamics

$$\begin{aligned} \dot{\tau} = 1/\varepsilon &=: F_0(z_0) \qquad && (x,z_0,\hat{\theta}) \in C_0 \\ \tau^+ = 0 \quad &=: G_0(z_0) && (x,z_0,\hat{\theta}) \in D_0 \end{aligned}$$

$$\kappa_0(x,z_0,\hat{\theta}) := \begin{cases} 1 & \text{if} \quad \tau < d(x,\hat{\theta}) \\ \{1,0\} & \text{if} \quad \tau = d(x,\hat{\theta}) \\ 0 & \text{if} \quad \tau > d(x,\hat{\theta}) \end{cases} \tag{20}$$

where $C_0 := \mathcal{X}_P \times [0,1] \times \mathbb{R}^2_{>0}$ and $D_0 := \mathcal{X}_P \times \{1\} \times \mathbb{R}^2_{>0}$.

Each solution $(t,j) \mapsto \tau(t,j)$ to $\mathcal{H}_0$ represents a timer that counts continually with a rate of $1/\varepsilon$ and resets to zero each time $\tau = 1$. The output κ_0 is a square wave representing the PWM signal that determines the converter switch state. The parameter $\varepsilon > 0$ represents the PWM period.

To ensure validity of the linearization in (17), and that the converter operates only in the continuous conduction mode under the local controller, we define the set $\mathcal{X}_{\mathcal{L}} := \mathcal{L} \cap \Pi$. Then, since the matrix $A_{\rm cl}(\hat{\theta})$ in (19) is Hurwitz for each $\hat{\theta}$, there exists an open set[3] $\mathcal{B}_{\mathcal{A}_P} \subset \mathcal{X}_{\mathcal{L}}$ containing a neighborhood of $\mathcal{A}_P$ that is forward invariant for (19).

Next, we establish the following proposition, which states the stability properties of the closed-loop local controller.

Proposition 4.5. *Consider the interconnection of the plant $\mathcal{H}_P$ in (2) with $c,L,R,E > 0$, local controller $\mathcal{H}_0$ in (20) with $\varepsilon > 0$, and parameter estimator $\mathcal{H}_E$ with $K(x,q) = k + \frac{1}{4}f_2(x,q)\Omega f_2^\top(x,q)$, where $k > \frac{1}{4}I$ and $\Omega = \Omega^\top > 0$. Given a desired set-point voltage $v_c^* > E$ and a compact set $\Delta \subset \Pi \times \mathcal{X}_0 \times \mathcal{X}_E$, with Π given in (14), that is forward invariant for the interconnection, there exists $\mu > 0$ in (8) such that, for each maximal solution $\phi = (x,z_0,z_E)$ to the interconnection with $\phi(0,0) \in \Delta$, there exists a hybrid time $(t',j') \in \operatorname{dom}\phi$ such that $\phi(t',j') \in \Pi \times \mathcal{X}_0 \times \mathcal{A}_E$, with $\mathcal{A}_E$ given in (10). Furthermore, there exists $\beta \in \mathcal{KL}$ such that, for each compact set $\Upsilon \subset \mathcal{B}_{\mathcal{A}_P}$ and each $\nu > 0$, there exists $\varepsilon^* > 0$ guaranteeing the following property: for each $\varepsilon \in (0,\varepsilon^*]$ defining F_0 in (20), every solution ϕ to the interconnection with $\phi(0,0) \in \Upsilon \times \mathcal{X}_0 \times \mathcal{A}_E$ is such that, for all $(t,j) \in \operatorname{dom}\phi$, its x component satisfies*

$$|x(t,j)|_{\mathcal{A}_P} \le \beta(|x(0,0)|_{\mathcal{A}_P}, t+j) + \nu. \tag{21}$$

Sketch of Proof: Assumption 4.2 holds for every maximal solution with $\phi(0,0) \in \Delta$. Then, from Proposition 4.3 we have $\hat{\theta} = \theta$ in finite time, and the stability result follows from (Teel and Nešić, 2010, Theorem 2). □

4.4 Uniting control algorithm

To implement the uniting control framework, the supervisor logic outlined in Section 3 is applied to the interconnection of the boost converter plant $\mathcal{H}_P$ using the global and local control algorithms $\mathcal{H}_1$ and $\mathcal{H}_0$, respectively. Recall that z_0 is the state of $\mathcal{H}_0$, z_1 is the state of $\mathcal{H}_1$, and the output κ of the selected controller is mapped to the input q of $\mathcal{H}_P$. Then, we define the hybrid system $\mathcal{H}$ with state $\xi = (x,z_0,z_1,p) \in \mathcal{X} := \mathcal{X}_P \times \mathcal{X}_0 \times \mathcal{X}_1 \times \{0,1\}$, input $\hat{\theta} \in \mathbb{R}^2_{>0}$, and dynamics

$$\begin{aligned} \dot{\xi} &\in F(\xi,\hat{\theta}) \qquad && (\xi,\hat{\theta}) \in C \\ \xi^+ &\in G(\xi) && (\xi,\hat{\theta}) \in D. \end{aligned} \tag{22}$$

The logic variable $p \in \{0,1\}$ is set to 0 when the global controller is selected and to 1 when the local controller is selected. The flow map F is equal to $(F_P,F_0,0,0)$ when $p = 0$ and to $(F_P,0,F_1,0)$ when $p = 1$. It is written concisely as

$$F(\xi,\hat{\theta}) := \begin{bmatrix} F_P(x,\kappa_p(x,z_p,\hat{\theta})) \\ (1-p)\ F_0(z_0) \\ p\ F_1(z_1) \\ 0 \end{bmatrix}.$$

The flow set C is given by

$$\begin{aligned} C := \big\{(\xi,\hat{\theta}) \in \mathcal{X} \times \mathbb{R}^2_{>0} : {} & (x,\kappa_p(x,z_p,\hat{\theta})) \in C_P, \\ & (x,z_0,\hat{\theta}) \in C_0, (x,z_1,\hat{\theta}) \in C_1, \\ & (x,p) \in \big(\overline{\mathcal{M}} \times \{0\}\big) \cup \big(\overline{\mathbb{R}^n \setminus \mathcal{N}} \times \{1\}\big)\big\}. \end{aligned}$$

where the sets $\mathcal{N}$ and $\mathcal{M}$ are to be designed.

The jump map G permits jumps by G_0 when $p = 0$ and by G_1 when $p = 1$, and toggles the value of p based on the converter state x in relation to the sets $\mathcal{N}$ and $\mathcal{M}$. This is expressed as[4]

$$G(\xi) := \begin{cases} G^0(\xi) & \xi \in D^0 \setminus D^2 \\ G^1(\xi) & \xi \in D^1 \setminus D^2 \\ G^2(\xi) & \xi \in D^2 \setminus (D^0 \cup D^1) \\ \big\{G^0(\xi), G^2(\xi)\big\} & \xi \in D^0 \cap D^2 \\ \big\{G^1(\xi), G^2(\xi)\big\} & \xi \in D^1 \cap D^2 \end{cases}$$

where $G^0(\xi) := (x,G_0(z_0),z_1,p)$, $G^1(\xi) := (x,z_0,G_1(z_1),p)$, $G^2(\xi) := (x,z_0,z_1,1-p)$, and the jump set is given by $D := D^0 \cup D^1 \cup D^2$ with

$$\begin{aligned} D^0 &:= \big\{(\xi,\hat{\theta}) \in \mathcal{X} \times \mathbb{R}^2_{>0} : (x,z_0,\hat{\theta}) \in D_0, p = 0\big\} \\ D^1 &:= \big\{(\xi,\hat{\theta}) \in \mathcal{X} \times \mathbb{R}^2_{>0} : (x,z_1,\hat{\theta}) \in D_1, p = 1\big\} \\ D^2 &:= \big\{(\xi,\hat{\theta}) \in \mathcal{X} \times \mathbb{R}^2_{>0} : \\ &\qquad (x,p) \in \big(\overline{\mathbb{R}^n \setminus \mathcal{M}} \times \{0\}\big) \cup \big(\mathcal{N} \times \{1\}\big)\big\}. \end{aligned}$$

Next we will design the uniting control sets $\mathcal{N}$ and $\mathcal{M}$.

5. UNITING CONTROL SETS AND MAIN RESULT

Any sets $\mathcal{N}$ and $\mathcal{M}$ that satisfy Assumption 3.1 are acceptable for the uniting control framework in (22). We provide one example of how these sets can be designed for the boost converter. We define the closed set $\mathcal{N}$ as a ball given by

$$\mathcal{N} := x^*(\hat{\theta}) + r_{\mathcal{N}}\mathbb{B} \tag{23}$$

where $r_{\mathcal{N}} \in \mathbb{R}_{>0}$ is chosen such that $\mathcal{N} \subset \mathcal{B}_{\mathcal{A}_P}$. Then, we choose ρ in (12) such that each maximal solution to the closed-loop global controller converges to $\mathcal{N}$. The choice of a ball for $\mathcal{N}$ is arbitrary and was done for simplicity.

[3] The set $\mathcal{B}_{\mathcal{A}_P}$ is the basin of attraction for (19) (Goebel et al., 2012, Definition 7.3).

[4] The jump maps associated with the sets $D^0 \cap D^2$ and $D^1 \cap D^2$ are necessary to satisfy outer semicontinuity of G in (Goebel et al., 2012, Assumption 6.5).

The reachable set from $\mathcal{N}$ may be computed, for example, via Poisson analysis as in (Almer et al., 2007). However, since this technique is computationally intensive for real-time implementation, we approximate $\mathcal{M}$ using the linearized model (19). A rigorous analysis of this approximation is beyond the scope of the paper. Using the Lyapunov function $\widetilde{V}(\tilde{x}) := \tilde{x}^\top P\tilde{x}$, where $P = P^\top > 0$ solves $A_{\text{cl}}^\top(\hat{\theta})P + PA_{\text{cl}}(\hat{\theta}) = -Q$ and $Q = Q^\top > 0$, we choose a parameter $r_0 \in \mathbb{R}_{>0}$ such that $L_{\widetilde{V}}(r_0) \supset \mathcal{N}$. Then, solutions to (19) from $\mathcal{N}$ remain inside $\widetilde{\mathcal{M}} := L_{\widetilde{V}}(r_0)$.

To bound the trajectories of the closed-loop local controller, points on the boundary of $\widetilde{\mathcal{M}}$ are parameterized in a grid such that the variation in the vector field F_P between adjacent points is small. Since the converter switch remains in one state for at most ε seconds during each PWM period, we compute the finite-time reachable set from each point on the boundary of $\widetilde{\mathcal{M}}$ by integrating F_P for ε seconds for each $q \in \{0, 1\}$. Then, $\mathcal{M}$ is defined as

$$\mathcal{M} := \text{int}\big(L_{\widetilde{V}}(r_{\mathcal{M}})\big) \tag{24}$$

where $r_{\mathcal{M}} \in \mathbb{R}_{>0}$ is chosen such that $\mathcal{M}$ bounds the set reachable in ε seconds from $\widetilde{\mathcal{M}}$ for each switch state $q \in \{0, 1\}$. Finally, we choose the matrix function K in (18) and the parameter $\varepsilon > 0$ in (20) so that $\mathcal{M} \subset \mathcal{X}_{\mathcal{L}}$.

Next, we establish our main result, which states the stability properties of the closed-loop uniting controller.

Theorem 5.1. *Consider the interconnection of the hybrid system $\mathcal{H}$ in (22) with $c, L, R, E > 0$, $k_0, k_1 \in (0, 1)$, $\rho > 0$, $\varepsilon > 0$, and parameter estimator $\mathcal{H}_E$ in (8) with $K(x, q) = k + \frac{1}{4}f_2(x, q)\Omega f_2^\top(x, q)$, where $k > \frac{1}{4}I$ and $\Omega = \Omega^\top > 0$. Given a desired set-point voltage $v_c^* > E$, uniting control sets $\mathcal{N}$ and $\mathcal{M}$ satisfying Assumption 3.1, and a compact set $\Delta \subset \Pi \times \mathcal{X}_0 \times \mathcal{X}_1 \times \{0, 1\} \times \mathcal{X}_E$, with Π given in (14), that is forward invariant for the interconnection, there exists $\mu > 0$ in (8) such that, for each maximal solution $\phi = (x, z_0, z_1, p, z_E)$ to the interconnection with $\phi(0, 0) \in \Delta$, there exists a hybrid time $(t', j') \in \text{dom}\,\phi$ such that $\phi(t', j') \in \Pi \times \mathcal{X}_0 \times \mathcal{X}_1 \times \{0, 1\} \times \mathcal{A}_E$, with $\mathcal{A}_E$ given in (10). Furthermore, there exists $\beta \in \mathcal{KL}$ such that, for each compact set $\Upsilon \subset \mathbb{R}^2$ and each $\nu > 0$, there exist $\rho^*, \varepsilon^* > 0$ guaranteeing the following property: for each $\rho \in (0, \rho^*]$ defining C_1 and D_1 in (12) and each $\varepsilon \in (0, \varepsilon^*]$ defining F_0 in (20), every solution ϕ to the interconnection with $\phi(0, 0) \in \Upsilon \times \mathcal{X}_0 \times \mathcal{X}_1 \times \{0, 1\} \times \mathcal{A}_E$ is such that, for all $(t, j) \in \text{dom}\,\phi$, its x component satisfies*

$$|x(t, j)|_{\mathcal{A}_P} \leq \beta(|x(0, 0)|_{\mathcal{A}_P}, t + j) + \nu \tag{25}$$

and such solutions exhibit no more than two toggles in the value of the solution component p.

Sketch of Proof: The stability result follows from Propositions 4.4 and 4.5. The value of p can be shown to toggle at most twice by analysis of the trajectories from the sets $\mathcal{N}$ and $\mathcal{M} \setminus \mathcal{N}$ (see (Sanfelice, 2021, Theorem 4.6)). $\square$

6. SIMULATION RESULTS

In this section, we present simulation results for the interconnection of $\mathcal{H}$ and $\mathcal{H}_E$. Simulations are performed using the Hybrid Equations Toolbox (Sanfelice et al., 2013) with $c = 0.1$F, $L = 0.2$H, $P = \begin{bmatrix} c/2 & 0 \\ 0 & L/2 \end{bmatrix}$, $\varepsilon = 0.0001$, $\rho = 0.001$, $\mu = 0.001$, and $\mathcal{A}_P = (7,\ 3.27)$. The set $\mathcal{N}$ in (23) is defined with $r_{\mathcal{N}} = 0.05v_c^*$, and a grid of 10 points is used to compute $\mathcal{M}$ in (24) from $\widetilde{\mathcal{M}}$. Initial conditions are $x_0 = (3, 6)$, $E_0 = 6$, $R_0 = 3.6$, $\hat{R}_0 = 3$, $\hat{E}_0 = 5$, as shown in Figure 1.[5] Both parameter estimates converge at 0.5 seconds. They converge again when E changes at $t = 3$ and when R changes at $t = 5$. The plant state converges to a neighborhood of $\mathcal{A}_P$ following each convergence of the parameter estimate to the true value.

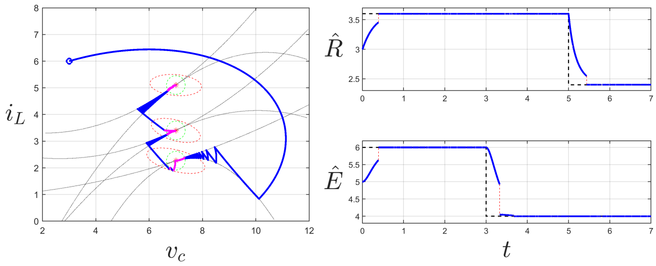

Fig. 1. Left: trajectories under $\mathcal{H}_1$ shown in blue and $\mathcal{H}_0$ in magenta. Right: parameter estimates $\hat{R}$ and $\hat{E}$.

REFERENCES

Almer, S., Jonsson, U., Kao, C., and Mari, J. (2007). Stability analysis of a class of PWM systems. *IEEE Transactions on Automatic Control*, 52(6), 1072–1078.

Bellur, D.M. and Kazimierczuk, M.K. (2007). DC-DC converters for electric vehicle applications. In *2007 Electrical Insulation Conference and Electrical Manufacturing Expo*, 286–293.

Goebel, R., Sanfelice, R.G., and Teel, A.R. (2012). *Hybrid Dynamical Systems: Modeling, Stability, and Robustness*. Princeton University Press, New Jersey.

Hartman, M., Bauer, N., and Teel, A.R. (2012). Robust finite-time parameter estimation using a hybrid systems framework. *IEEE Transactions on Automatic Control*, 57(11), 2956–2962.

Kassakian, J., Schlecht, M., and Verghese, G. (1991). *Principles of Power Electronics*. Addison-Wesley series in electrical engineering. Addison-Wesley.

Li, Y. and Sanfelice, R.G. (2019). Finite time stability of sets for hybrid dynamical systems. *Automatica*, 100, 200–211.

Sanfelice, R.G., Copp, D.A., and Nanez, P. (2013). A toolbox for simulation of hybrid systems in Matlab/Simulink: Hybrid Equations (HyEQ) Toolbox. In *Proceedings of Hybrid Systems: Computation and Control Conference*, 101–106.

Sanfelice, R. (2021). *Hybrid Feedback Control*. Princeton University Press, New Jersey.

Teel, A.R. and Kapoor, N. (1997). Uniting local and global controllers. In *1997 European Control Conference (ECC)*, 3868–3873.

Teel, A.R. and Nešić, D. (2010). Pwm hybrid control systems: averaging tools for analysis and design. In *2010 IEEE International Conference on Control Applications*, 1128–1133.

Theunisse, T.A.F., Chai, J., Sanfelice, R.G., and Heemels, M. (2015). Robust global stabilization of the DC-DC boost converter via hybrid control. *IEEE Transactions on Circuits and Systems I*, 62, 1052–1061.

Vasca, F. and Iannelli, L. (2012). *Dynamics and Control of Switched Electronic Systems*. Advances in Industrial Control Series, Springer Verlag, Berlin, Germany.

[5] Code at https://github.com/HybridSystemsLab/UnitingBoost